

CZECH TECHNICAL UNIVERSITY IN PRAGUE



DOCTORAL THESIS STATEMENT

Czech Technical University in Prague
Faculty of Electrical Engineering
Department of Control Engineering

Martin Řezáč

Inertial stabilization, estimation and visual servoing for aerial surveillance

Ph.D. Programme: Electrical Engineering and Information Technology
Branch of study: Control Engineering and Robotics

Doctoral thesis statement for obtaining the academic title of "Doctor",
abbreviated to "Ph.D."

Prague, November 2013

The doctoral thesis was produced in full-time manner Ph.D. study at Department of Control Engineering of the Faculty of Electrical Engineering of CTU in Prague

Candidate Ing. Martin Řezáč
 Katedra řídicí techniky
 Fakulta elektrotechnická ČVUT
 Technická 2, 166 27 Praha 6

Supervisor Ing. Zdeněk Hurák, Ph.D.
 Katedra řídicí techniky
 Fakulta elektrotechnická ČVUT
 Technická 2, 166 27 Praha 6

Oponents

The doctoral thesis statement was distributed on

The defence of the doctoral thesis will be held on at a.m./p.m. before the Board for the Defence of the Doctoral Thesis in the branch of study *Control Engineering and Robotics* in the meeting room No. of the Faculty of Electrical Engineering of the CTU in Prague.

Those interested may get acquainted with the doctoral thesis concerned at the Dean Office of the Faculty of Electrical Engineering of the CTU in Prague, at the Department for Science and Research, Technická 2, Praha 6.

Prof. Ing. Michael Šebek, DrSc.
Chairman of the Board for the Defence of the Doctoral Thesis
in the branch of study
Control Engineering and Robotics
Faculty of Electrical Engineering of the CTU in Prague, Technická 2, 166 27 Prague 6.

Full list of the author's publications

Profile at Google scholar: <http://scholar.google.cz/citations?user=A-QXLN4AAAAJ>

- Count of citations (autocitations excluded) according to SCI marked by *SCI*, according to Google scholar are marked by *G*.
- All citation counts are stated here to the date of this thesis submission.
- *IF* represent journal's ISI Impact Factor at the year of publishing of the paper (or the last known in case the paper is under review).
- *P* denotes my participation on the appropriate publication in percent.

PUBLICATIONS RELATED TO THIS THESIS

Publications in journals with nonzero IF (incl. submitted)

Z. Hurák, M. Řezáč, "Image-Based Pointing and Tracking for Inertially Stabilized Airborne Camera Platform," in *IEEE Transactions on Control Systems Technology*, vol. 20, no. 5, pp. 1146 – 1159, Sep. 2012,

IF:2, G:9, SCI:1, P:50%.

M. Řezáč, Z. Hurák, "Structured MIMO \mathcal{H}_∞ Design for Dual-Stage Inertial Stabilization: Case Study for HIFOO and Hinfstruct Solvers," in *Mechatronics*, vol. 23, no. 8, pp. 1084 - 1093, 2013,

IF:1.3, G:0, SCI:0, P:50%.

M. Řezáč, Z. Hurák, "Delay compensation in dual-rate cascade visual servomechanisms: reset observer, modified Smith predictor and lifting approaches," **Submitted to** *Control engineering practice* journal ISSN: 0957-4158 on 16th January 2013,

IF:1.669, G:0, SCI:0, P:50% .

Publications in other journals

Z. Hurák, M. Hromčík, M. Řezáč, J. Žoha, P. Krsek, et al., "Inerciálně stabilizovaná kamerová základna pro bezpilotní letoun," in *Automa*, vol. 14, no. 10, pp. 27-31. 2008,

G:0, SCI:0, P:10%.

Conference publications presented on conferences listed on WoS

Z. Hurák, M. Řezáč, "Delay compensation in a dual-rate cascade visual servomechanism," in *Proc. of the 49th Conference on Decision and Control*, Atlanta, GA, USA, December 2010,

G:4, SCI:0, P:50%

Z. Hurák, M. Řezáč, "Combined line-of-sight inertial stabilization and visual tracking: application to an airborne camera platform," in *Proc. of the 48th IEEE Conference on Decision and Control*, Shanghai, China, December 2009,

G:1, SCI:0, P:50%.

M. Řezáč, Z. Hurák, “Structured mimo \mathcal{H}_∞ design for dual-stage inertial stabilization: Case study for hifoo,” in *18th IFAC World Congress*, vol. 18, no. 1, 2011, pp. 7456–7461,
G:1, SCI:0, P:50%.

M. Řezáč, Z. Hurák, “Vibration rejection for inertially stabilized double gimbal platform using acceleration feedforward,” in *2011 IEEE International Conference on Control Applications (CCA)*. IEEE, Sep. 2011, pp.363–368,
G:2, SCI:1, P:50%.

Other publications

Z. Hurák, M. Řezáč, “Control design for image tracking with an inertially stabilized airborne camera platform,” in *Proc. of SPIE Deference, Security, and Sensing 2010*, Orlando, Florida, USA, April 2010,
G:1, SCI:0, P:50%.

M. Řezáč, Z. Hurák, “Low-cost inertial estimation unit based on extended Kalman filtering,” in *Proc. of SPIE Deference, Security, and Sensing 2010*, vol. 7696. Orlando, Florida, USA: SPIE, Apr. 2010, pp. 76 961F–10. [Online],
G:1, SCI:0, P:50%.

M. Řezáč, J. Žoha, T. Haniš, “Line-of-sight stabilization of an airborne camera system,” in *2008 PEGASUS-AIAA Student Conference [CD-ROM]*, Prague: Czech Technical University, 2008,
G:0, SCI:0, P:33%.

Z. Hurák, M. Řezáč, P. Krsek, K. Zimmermann, V. Hlaváč, et al., “Inerciálně stabilizovaná kamerová základna pro bezpilotní letoun s automatickým sledováním pozemních cílů,” in *2nd Conference for Unmanned Aerial Systems [CD-ROM]*, Praha: FSI ČVUT, 2010,
G:0, SCI:0, P:20%.

PUBLICATIONS NOT RELATED TO THIS THESIS

Conference publications presented on conferences listed in WoS

M. Řezáč, Z. Hurák, “Towards array micromanipulators based on dielectric elastomers, in *Nanocon 2009 Conference Proceedings [CD-ROM]*, Ostrava: TANGER, spol.s r.o, 2009, ISBN 978-80-87294-13-0,
G:0, SCI:0, P:50%.

Other Publications

M. Řezáč, Z. Hurák, “Towards planar micromanipulators based on dielectric elastomers in thickness mode,” in *Proceedings of the 12th International Conference on New Actuators [CD-ROM]*, Bremen, 2010, p. 901-904. ISBN 978-3-933339-12-6,
G:0, SCI:0, P:50%.

1 INTRODUCTION AND PROBLEM STATEMENT

The typical scenario that is studied in the thesis from various control engineering viewpoints and which is coming through the most of chapters may be described using Fig. 1 as follows.

Having an optical system (optical camera, laser rangefinder) mounted onto a mobile carriers such as unmanned aircrafts, helicopters or trucks, the aim of the system is to ensure that optical axis of the optical system is stationary in the inertial space even when the carrier of the camera is a subject to an unwanted and usually unpredictable movement or some other disturbing phenomena like wind-induced torque are acting. The requirement for keeping the commanded optical axis stationary is in the literature usually denoted as a *Line-of-sight inertial stabilization*. The device that is performing the line-of-sight stabilization will be denoted in this thesis as the *inertially stabilized platform*.

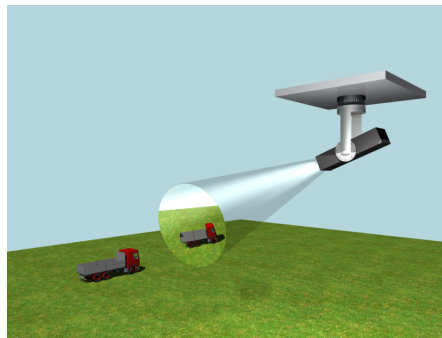


Figure 1: Typical scenario for the inertial stabilization system. Some optical device (in this case the camera) is providing a surveillance of the ground target while the carrier of the camera is subject to disturbing movement.

When the optical system to be inertially stabilized is the camera, several more advanced features such as the image based tracking may be implemented with the stabilized platform. The incorporation of the camera in the feedback loop is significance of research area called *Visual servoing*. The algorithm that is processing the camera signal (image tracker) usually works with low sampling rate with the addition of one sampling period delay. This delay in the feedback loop calls for research of *Delay compensation* in visual servoing.

1.1 Projects solved at CTU

The development of the stabilized platforms at CTU started in 2007 when Czech Air Force and Air Defence Technological Institute (Vojenský technický ústav letectva a PVO, with the acronym VTÚL) contacted Czech Technical University with a contract on developing of an inertially stabilized platform within a grant of Ministry of Industry and Trade of the Czech Republic. During few years a first working concept has been successfully developed and experimentally tested (platform in Fig.2 in the middle). In the following years the team succeeded in gaining another grant with a title "dual-stage stabilization system"¹. The coordinator of this project was VTÚL with another two partners – Czech Technical University (departments of control engineering and center for machine perception) and local company ESSA. The role of CTU in the project was the development of algorithms for inertial stabilization and realtime target tracking with complete hardware implementation

¹grant code is TIP FR-TI1/265

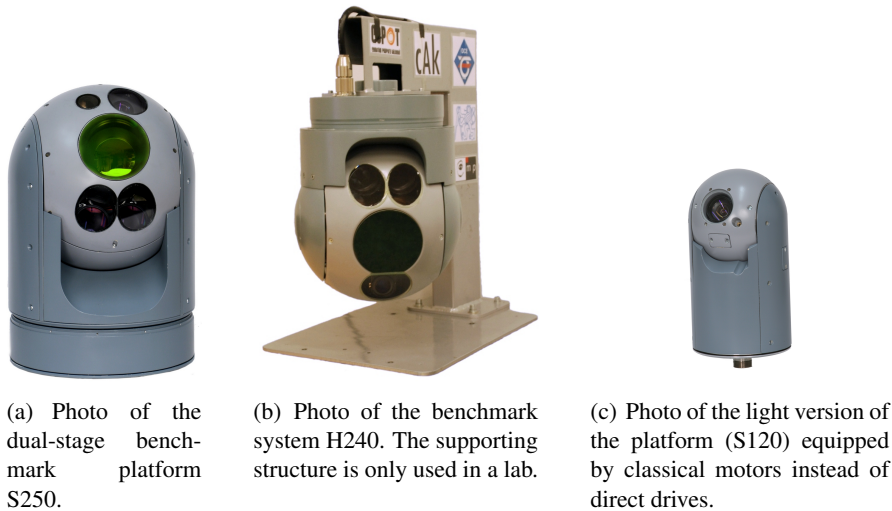


Figure 2: Both platforms were developed by Czech Air Force and Air Defense Technological Institute in collaboration with Czech Technical University in Prague and Essa company.

including design, programming and production. The role of the ESSA company was the design and production of the mechanical configuration of the platform. This project was finished in 2011. As a result the prototype of the stabilized platform was developed and experimentally tested (platform in Fig.2 on the left).

1.2 State of the art

1.2.1 Academic publications

The design of control systems for stabilization of the line of sight of the optical payload was extensively studied by the engineering community during past decades but it is not always easy to document the history of this defense-related engineering discipline purely from academic publications. An up-to-date survey can be found in the February 2008 issue of the *IEEE Control Systems Magazine*, where the whole issue was dedicated to the topic of "Inertially stabilized platform technology".

The most focused regular forum for discussion of technical issues related to inertial stabilization for aerial applications seems to be *SPIE Defense, Security, and Sensing* conference held every year. Some interesting papers can be found in their proceedings or in one of the journals published by SPIE, in particular *Optical Engineering*.

Since this thesis includes a collection of research results that are only loosely related by the common goal, it is convenient to place the particular state-of-the-art sections in appropriate chapters.

1.2.2 Commercial products

There are several companies engaging the production of inertially stabilized platforms. Among the most well-known belong companies like FLIR, WESCAM or Cloud Cap Technology. Parameters and the equipment of their products are varying depending on the picked model. What is common for all of them is the brevity in technology principles description and obviously no information at

all about the algorithms inside which belongs to proprietary know-how. Section 1.3.2 in the thesis provides a deeper analysis of products available on the market.

1.3 Contribution of the thesis

The main contribution of the proposed thesis resides in chapters 4,5 and 6. They deal with the design of the line-of-sight inertial stabilization and the design of the image-based feedback with application to inertially stabilized platforms.

During control design for developed stabilized platforms author and the supervisor of the thesis took an inspiration in the above mentioned issue of IEEE Control Magazine, specially in the survey paper [1]. None of the works cited therein though deals with the topic of how to extend line-of-sight stabilization for (an image based) pointing and tracking. Since this task showed up to be not completely straightforward, the gap created an opportunity to be fulfilled by the following paper by the author and the supervisor

Z. Hurák and M. Řezáč, “Image-based pointing and tracking for inertially stabilized airborne camera platform,” *IEEE Transactions on Control Systems Technology*, vol. 20, no. 5, pp. 1146 –1159, Sep. 2012.

The other topic that further represents significant contribution of the thesis resides in solving issues that appear in the image-based tracking due to the time delay caused by real-time video processing in feedback. The topic is rigorously studied in chapter 6 of the thesis and in the paper

Z. Hurák and M. Řezáč, “Delay compensation in a dual-rate cascade visual servomechanism,” in *Proc. of the 49th IEEE Conference on Decision and Control*, Atlanta, GA, USA, December 2010. .

The last topic where the main contribution of this thesis is claimed resides in the section 4.2 of the thesis. The section presents an approach to how-to design the low-order controller with pre-described structure using \mathcal{H}_∞ formalism. The topic presented as a case study was published in the IFAC Mechatronics journal paper

M. Řezáč, Z. Hurák, “Structured MIMO \mathcal{H}_∞ Design for Dual-Stage Inertial Stabilization: Case Study for HIFOO and Hinfstruct Solvers,” in *Mechatronics*, vol. 23, no. 8, pp. 1084 - 1093, 2013

1.3.1 Other significant publications by the author that are related to the thesis

- The topic of the extension of the line-of-sight stabilization for image based pointing and tracking was studied in IEEE conference paper [2] and SPIE conference paper [3]. Suggestion obtained at these two events were complemented by laboratory experiments and published in IEEE Transactions journal (the citation is stated already in previous section).
- The flight experiments with one of developed platforms mounted underneath a helicopter proved, that presence of linear vibrations with having at the same time unbalanced camera gimbal can create unwanted disturbing torque that is disrupting the line-of-sight. Results that were achieved with an application of the accelerometer based feedforward vibration rejection scheme in line-of-sight stabilization were presented at IEEE conference [4].
- Finally the last of publications that is relevant for the thesis is a SPIE conference paper [5] that presents an implementation of the attitude estimation based on the extended Kalman filtering.

1.4 Some other means of presentation

The results achieved by the whole project consortium in the domain of the inertial stabilization were presented not only to the academic community by means of research papers and to the industrial community by means of participation at fair trades (International Engineering Fair (MSV) in Brno, International Fair of Defence and Security Technology (IDET) in Brno), but it was also presented to a wide public in one episode of the popular Czech TV show called PORT broadcasted by Czech television (ČT1 channel). The episode was focused on inertial stabilization of cameras. The URL link to the video is listed in the appendix of the thesis.

2 LINE-OF-SIGHT INERTIAL STABILIZATION

The very basic control task for steerable cameras or antennas mounted on mobile carriers such as trucks, unmanned aircrafts or ships, is to keep the commanded line of sight (optical axis) still even in presence of various disturbing phenomena like mass imbalance, aerodynamic (or wind-induced) torque and possible kinematic coupling between gimbal axes. This section presents a control design for a double gimbal mechanical configuration. The corresponding chapter 4 in the thesis contains moreover a control design considerations for other configurations such as dual-stages configurations.

2.1 Inertial line-of-sight stabilization on mobile carriers

Motivated also by defence technological needs, the topic of inertial stabilization was studied extensively in the past few decades. Several relevant papers from 1970s through 1990s were archived in the selection [6]. Dedication of a full issue of *IEEE Control System Magazine* (February 2008) featuring nice survey papers [7], [1] and [8] confirms that the topic is still relevant for the engineering community. Another recent issue of the same journal brings a rigorous analysis of control problems related to a standard double gimbal system [9], though it is not directly applicable to inertial stabilization.

2.2 Double gimbal inertial stabilization

The mathematical model of the double gimbal is thoroughly studied in the thesis in section 4.1. This text uses the formalism introduced therein. The configuration is sketched in Fig. 3. In order to make the line of sight insensitive to external disturbances, a simple controller structure can be used. Two decoupled SISO inertial rate controllers suffice, one for each measured (component of the) inertial angular rate. Namely,

- the inertial angular rate ω_{Ey} (also denoted with the mnemotechnic ω_{EL}) of the payload about the axis of the elevation motor (camera elevation rate),
- and the inertial angular rate ω_{Ez} of the payload around its own vertical axis, also nicknamed camera cross-elevation rate (and denoted ω_{CEL}) since its axis is always orthogonal to the ω_{EL} axis.

It is clear from Fig. 3 that the cross-elevation controller must include a secant gain correction $1/\cos(\theta)$, because the motor in the azimuth gimbal cannot directly affect $\omega_{CEL}(= \omega_{Ez})$. It can only

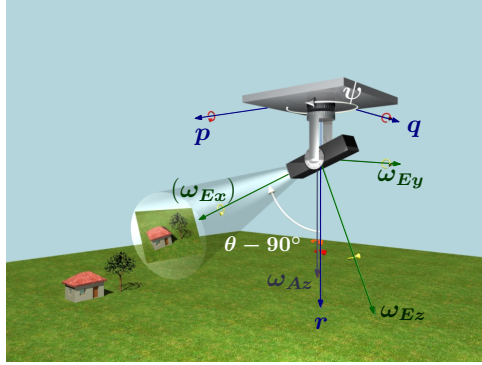


Figure 3: Basic scenario for inertial line-of-sight stabilization. Depicted in green are the components $\omega_{Ex}, \omega_{Ey}, \omega_{Ez}$ of the vector of inertial angular rate of the elevation frame (as measured by MEMS gyros attached to the camera), blue vectors p, q, r denote the rate components of the base (UAV here). The ω_{Az} component is attached to the outer gimbal (the other two components are not shown). Two white arcs denote the two relative angles. The origins of the coordinate frames are assumed to coincide in the computations.

do so indirectly through ω_{Az} . It is only when the camera is pointing to the horizon, that is, when $\theta = 0$, that $\omega_{Az} = \omega_{CEL}(= \omega_{Ez})$. This fact (thoroughly studied in [1]), may be explained also by using the following equation²

$$\omega_E^E = R_A^E \omega_E^A = \begin{bmatrix} c_\theta(p c_\psi + q s_\psi) - s_\theta(r + \dot{\psi}) \\ -p s_\psi + q c_\psi + \dot{\theta} \\ s_\theta(p c_\psi + q s_\psi) + c_\theta(r + \dot{\psi}) \end{bmatrix} = \begin{bmatrix} \omega_{Ex} \\ \omega_{Ey} \\ \omega_{Ez} \end{bmatrix}. \quad (1)$$

It is clear that to achieve the line of sight stabilization, both ω_{Ey} and ω_{Ez} must be zero. For this purpose $\dot{\theta}$ and $\dot{\psi}$ are available. While the impact of $\dot{\theta}$ on ω_{Ey} is direct, the impact of $\dot{\psi}$ on ω_{Ez} comes through the term $\cos(\theta)$. Thus this is just another explanation of the term $1/\cos(\theta)$ present in the cross-elevation controller. Block diagram of the control structure for cross-elevation axis is shown in Fig. 4.

Fig. 4 also represents important fact how disturbing rotational movement of the carrier $[p, q, r]$ enters the cross-elevation loop. It is only the r component that enters the loop only via azimuth gimbal's friction (and back emf, which is not shown in figure) and so that it is very well rejected by the mass stabilization principle. The remaining components p, q enter the loop directly via the corresponding projection. When the elevation angle θ is not zero, these signals always enter the loop directly, and may be rejected only by applying feedback control action with always limited bandwidth.

In case of the elevation gimbal there are only two disturbing angular rates p and q that enter the loop, and they do so indirectly via friction in elevation gimbal. This fact guarantees that the line-of-sight is vertically (means the component ω_{Ey}) very well stabilized. The block diagram for elevation axis is in Fig. 4.

Even though there is some gyroscopic coupling between the two axes [10] and [11] for full models or [9] for the simplified version when the base is still), its influence is not worth designing a MIMO rate controller. This neglected gyroscopic effect can be cast as yet another external disturbing torque and as such left to the rate controller to suppress.

²equation is equivalent to equation (4.1) in the thesis

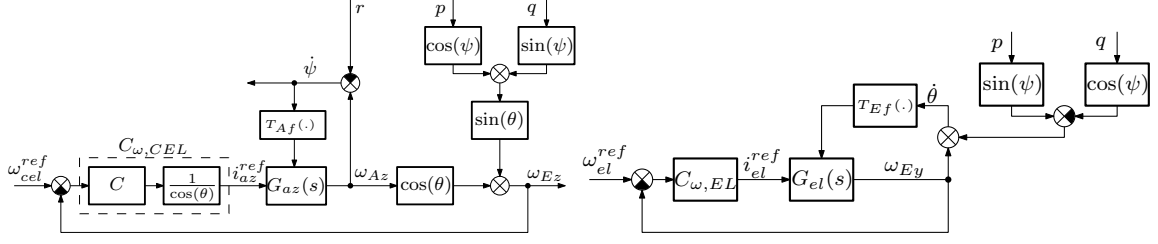


Figure 4: On the left: Inertial stabilization for the cross-elevation. The image is redrawn from [1]. $G_{az}(s)$ corresponds to azimuth part of gimbal dynamics with the current loop already closed. On the right: Inertial stabilization for the elevation. $G_{el}(s)$ corresponds to elevation part of gimbal dynamics with the current loop already closed.

In order to demonstrate the functionality of the line-of-sight stabilization and experimentally prove the suitability of the proposed decoupled control structure two experiments were performed. Their results are presented in the full version of the thesis in section 4.1.1.

3 VISUAL TRACKING ON TOP OF INERTIAL STABILIZATION

The literature cited in the introduction to the previous section 2.1 (including the references made therein) mostly focused on the task of inertial stabilization only. The issue of extending the inertial rate stabilizing feedback loop to visual tracking system is only dealt with at a rather simplistic level in [7] by suggesting the common cascaded control structure for every rotational degree of freedom: a single-input-single-output inner (inertial rate stabilization) loop is accepting commands from the output of the corresponding outer (visual tracking) loop. There are some pitfalls hidden in this decoupled approach, though. This section introduces the troubles that are encountered when using the classical double-gimbal platform or four-gimbal platform and presents a solution. Detailed derivation of the algorithm is stated in chapter 5 of the thesis. To the best of the author's knowledge, this is the first formal treatment of visual pointing and tracking for inertially stabilized camera systems.

The results presented in this section come from the paper [12]. Preliminary versions of that paper were presented at [2] and [3].

It is presented in chapter 4 of the thesis, that in motion control application it is usually useful to implement the cascade control structure – usually with three control loops. The most inner loop takes care of the motor's current, the middle loop takes care of the velocity and the outer loop is finally controlling the angle. The visual tracking algorithm that is presented in this section requires that inertial Line-of-sight stabilization control loop (= the velocity loop) is already designed and closed, and offers the inertial angular rate reference tracking within a specified bandwidth. The visual tracking is then built around such that visual controller can manipulate the line-of-sight by specifying the two reference inertial angular rates. In particular these are the reference angular rates $\omega_{Ey}^{ref} = \omega_{EL}^{ref}$ and $\omega_{Ez}^{ref} = \omega_{CEL}^{ref}$ for the classical double gimbal. To complete the notation, measured rotation around the optical axis is denoted by ω_{ROT} which is equal to ω_{Ex} in case of double gimbal.

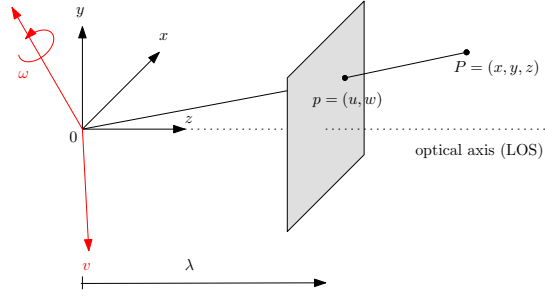


Figure 5: Coordinates of the object on the ground expressed in the coordinate frame attached to the camera and (after projection) in the image plane. Rotation $\omega_{R,C}^C$ and translation v_C of the camera frame within with respect to the inertial frame is also illustrated (redrawn from [13]).

3.1 Camera motion and the interaction matrix

The objects to be observed are located in the full 3D world while the camera can only record their 2D image. The coordinates of the object in the world (on the ground) expressed in the camera frame are given by $P = [x, y, z]^T$. Simplifying a bit the model of the optics, we make the so-called pinhole assumption, which defines the image coordinate frame according to Fig. 5.

Now consider the movement of the camera in the inertial space characterized by its linear and rotational velocities $v_C = [v_{Cx}, v_{Cy}, v_{Cz}]^T$ and $\omega_C = [\omega_{Cx}, \omega_{Cy}, \omega_{Cz}]^T$, both expressed in the camera frame. The motion of the object as viewed by the camera is described by the so-called image feature velocity $[\dot{u}(t)\dot{w}(t)]^T$. The nice thing is that it is possible to relate all of these velocities by a transform resembling the concept of Jacobian and denoted often an interaction matrix or image Jacobian. This matrix is derived in [13], page 415, equation (12.14) as

$$\begin{bmatrix} \dot{u} \\ \dot{w} \end{bmatrix} = \begin{bmatrix} -\frac{\lambda}{z} & 0 & \frac{u}{z} & \frac{uw}{\lambda} & -\frac{\lambda^2+u^2}{\lambda} & w \\ 0 & -\frac{\lambda}{z} & \frac{w}{z} & \frac{\lambda^2+w^2}{\lambda} & -\frac{uw}{\lambda} & -u \end{bmatrix} \begin{bmatrix} v_{Cx} \\ v_{Cy} \\ v_{Cz} \\ \omega_{Cx} \\ \omega_{Cy} \\ \omega_{Cz} \end{bmatrix}. \quad (2)$$

3.2 Decoupled pointing and tracking

Proceeding one step further the question of the most suitable feedback control configuration for automatic visual tracking pops up. Shall we use the immediate extension which closes a SISO tracking loop around the corresponding SISO inertial rate loop?

The cascade approach is justified: whereas the inner (inertial rate) loop aims to attenuate the disturbances at middle and high frequencies, the outer (pointing) loop should be active at low frequencies. This straightforward but naive solution is in Fig. 6.

Insisting on decoupled controllers is plausible from an implementation viewpoint. There is a trick hidden here, though, as seen in Fig. 7. The best way for explanation is using a double-gimbal platform. When the automatic computer vision tracker detects a regulation error in the horizontal direction in the image plane while seeing no error in vertical direction, the simple cascaded structure of Fig. 6 would command the azimuth motor only. This motor alone, however, cannot create a purely horizontal motion in the image plane when $\theta \neq 0$. A geometric explanation can be found in Fig. 3:

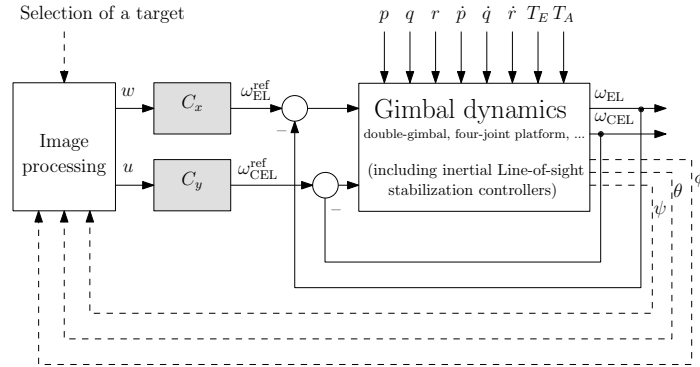


Figure 6: Naive pointing-tracking system formed by two SISO loops closed around two inertial rate stabilization loops. The dashed lines are not signals truly fed back to the pointing-tracking controller. These are variables representing orientation of the camera which affects the position and orientation of objects in the image plane.

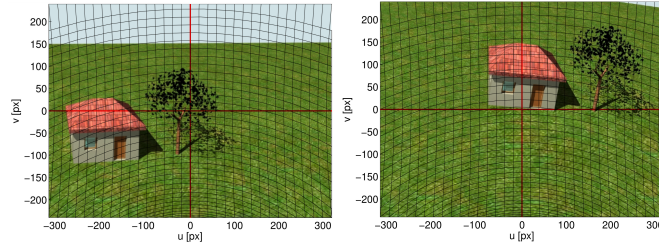


Figure 7: Illustration of how in an attempt to steer the camera such that the image of the roof of the house gets back to the middle of the field of view using azimuth motor only, the introduced rotation of the camera around its optical axis makes the horizontal movement curved. Consequently, correction in vertical direction using the elevation motor is needed. Curvilinear coordinate system in the image plane corresponds to the initial elevation of camera by $\theta = -54^\circ$ with respect to the body of the aircraft.

to steer the camera such that the image of an object moves horizontally in an image plane, one would need to command the cross-elevation inertial rate ω_{CEL} (denoted as ω_{Ez} in the figure). However, the motor can only affect the component of the inertial rate in the direction of the azimuth motor axis, that is, ω_{Az} . As soon as there is some misalignment between the two, that is, when the camera is tilted up or down to the ground while the aircraft is in level flight ($\theta \neq 0$), the vector oriented in the azimuth motor axis of length ω_{Az} has some nonzero projection ω_{Ex} to the camera optical axis. Consequently, some unwanted rotation of the image as well as vertical displacement are introduced.

3.3 Feedback linearization based pointing and tracking.

The key idea for an improvement described in the rest of this section is that the curvature of the coordinate axes as in Fig. 7 can be compensated for by measuring the third component of the inertial angular rate of the camera body, the one along its optical axis, the so far unused measurement $\omega_{Ex} = \omega_{ROT}$. Using this information, exact feedback linearization can be implemented in the controller following standard techniques from image-based visual servoing.

The idea behind image-based visual servoing is that an error "sensed" in the image plane by the

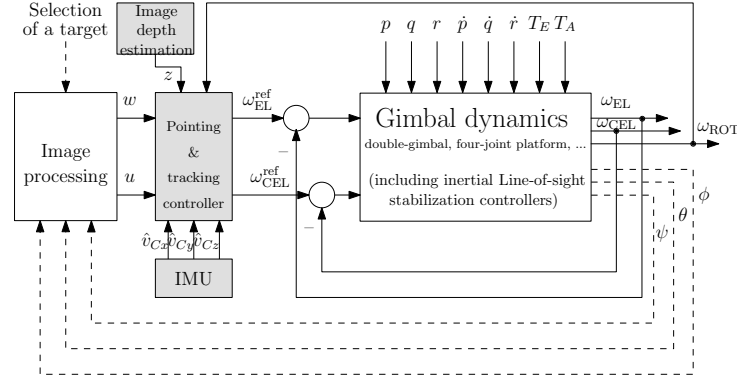


Figure 8: Full feedback system with an image-based pointing controller aware of the angular rate about the optical axis and the translational motion. The pointing-tracking controller implements (3) and (4).

image tracker can be eliminated by commanding a proper camera velocities. To find proper angular rates of the camera the inversion of the interaction matrix is used. Derivation of this feedback linearization scheme is shown in section 5.4 of the thesis. The result is the expressions for reference angular rates of the camera around elevation and cross-elevation axes

$$\omega_{EL}^{ref} = \frac{\alpha w \lambda}{\lambda^2 + u^2 + w^2} - \frac{\omega_{ROT} u}{\lambda} - \frac{\lambda^2 v_y - \lambda w v_z - u w v_x + u^2 v_y}{z(\lambda^2 + u^2 + w^2)}, \quad (3)$$

$$\omega_{CEL}^{ref} = -\frac{\alpha u \lambda}{\lambda^2 + u^2 + w^2} - \frac{\omega_{ROT} w}{\lambda} + \frac{\lambda^2 v_x - \lambda u v_z - w u v_y + w^2 v_x}{z(\lambda^2 + u^2 + w^2)}. \quad (4)$$

The expressions (3) and (4) for the controllers are structured such that three terms can be immediately recognized in each controller: a term corresponding to a regulation error in the corresponding axis as seen in the image plane, a term compensating for the rotation around the camera optical axis and finally a term attenuating the influence of mutual translational motion of the camera and the ground object.

Consider now the simplification that can take place in a situation $u, w \neq 0$ but small, λ large, and v_C is neglected. The general expression for the controller output then reduces to

$$\omega_{EL}^{ref} = \frac{\alpha w}{\lambda} - \frac{\omega_{ROT} u}{\lambda} \quad (5)$$

$$\omega_{CEL}^{ref} = -\frac{\alpha u}{\lambda} - \frac{\omega_{ROT} w}{\lambda} \quad (6)$$

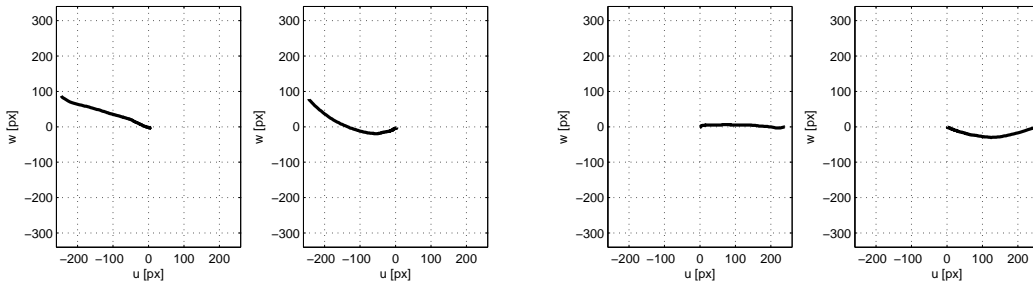
This reduced controller reveals the key enhancement with respect to the fully decoupled design: the controller output contains contribution from the angular rate of the camera around the optical axis!

3.4 Laboratory experiments

The benchmark system – the double-gimbal platform – was used to validate the functionality of the proposed control scheme and compare its performance with the intuitive decoupled controller. The experimental test was conducted in an indoor lab while the camera platform was carried by a fixed laboratory stand. Both the new and the original (naive) decoupled controllers were tested for

the sampling rate of 15 Hz of the automatic image tracker. The results of the two experiments are visualized in Figs. 9(a) and 9(b), the experimental data for the new algorithm always on the left and the data for the original decoupled scheme on the right.

Both experiments were quite similar: the platform was in both cases sitting peacefully on the desk. The position of the point to be tracked in the image plane was specified by manually clicking the object on the screen. The key difference between the old and new algorithms is that the new algorithm achieves a linear trajectory when bringing the target into the center of the image plane as desired.



(a) Experiment 1: Responses of image features for $\theta(0) = 65.5^\circ$, tracker sampling rate $f_{sp} = 15\text{Hz}$, $\alpha = 0.46$. Left: the proposed algorithm, right: the original decoupled approach.

(b) Experiment 2: Left: the proposed algorithm, right: the original decoupled approach. The initial elevation angle was set to $\theta(0) = 54^\circ$. The image tracker sampling rate $f_{sp} = 15\text{Hz}$. The controller parameter $\alpha = 0.46$.

Figure 9: Numerical simulations for two different initial conditions.

3.5 Experiment on a helicopter

Experimental verification of pointing&tracking was also tested in real life experiments. The platform was mounted underneath MI-17 helicopter during two test flights. The human operator, sitting inside the helicopter, was operating the platform using touchscreen device. This device allows manipulating the line-of-sight using joystick, zooming the camera, viewing the output video from the camera so as the current map with GPS coordinates, and of course specifying the target to be tracked by clicking on it. After specifying the target, it is pulled to the center of the camera view exactly as studied in this section. This proves the practical applicability of chosen laboratory experiments.

Printscreen pictures of the camera video from the system during operation are shown in Fig. 10. Some of these videos are included as an attachment in CD-ROM in the booklet of the thesis (see the list of attached videos at the end of the thesis).

4 DELAY COMPENSATION IN VISUAL SERVOING

The chapter 6 of the doctoral thesis presents few simple techniques for compensation of a one-sampling-period delay in a slow-sampled outer (position or angle) loop within a cascade visual servomechanism that also includes a fast-sampled inner (velocity) feedback loop. The results are mainly relevant for visual servoing applications, since the velocity sensors such as tachometers or MEMS-based gyros usually achieve much higher sampling rates compared to computer vision systems used as position (or orientation) sensors. The proposed solutions only compensate for the

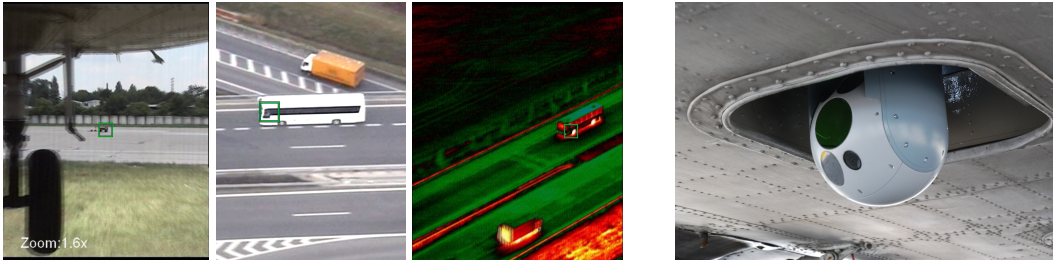


Figure 10: From the left – Several screenshots created from the recorded video of a target tracking during the flight experiment. Specifying the target is provided by a clicking the touchscreen device. The locked target is denoted by the green square – the aim of the control system is to keep this square (the target) in the center of the image. On the right – the platform mounted underneath MI-17 helicopter.

motion of the camera and not the observed object; they are particularly useful when the visual servoing is combined with inertial stabilization. The problem is solved using two different formalisms: first, the problem is cast as an instance of a reset system with periodic resetting of the observer state. Second, a technique based on the concept of a modified Smith compensator is proposed wherein the undelayed output of a mathematical model is replaced by the measured rate signal from the inner loop. Numerical simulations are used to highlight the behavior of the proposed algorithms. Finally experimental results obtained with a real double gimbal camera system are presented. The content of the chapter 6 of the doctoral thesis is based on the conference paper [14] and on the submitted version of the journal paper [15].

This section provides only a brief introduction to the problem and presents the main results. For detailed the derivation of all the results, the reader of this text is referred to the chapter 6 of the doctoral thesis.

4.1 Definition of the problem

A common control system configuration for numerous motion control applications is that of a two-level cascade: the upper level (or the outer feedback loop) keeps the error between the reference (desired) and true (measured) positions (or orientations or angles) small by setting the reference value for the velocity, which is tracked by the lower level controller (inner feedback loop). The class of cascade systems that are considered exhibits major disproportions between sampling rates of the inner and outer loops. Moreover, the outer loop contains a full one-sampling-period delay. This situation is typical of visual servoing applications, where the role of the position error sensor in the outer loop is played by a camera accompanied with a computer vision system. The algorithms used to extract information from the captured video frames usually devour some computational time, which not only sets the sampling rate for the outer loop relatively slow but also enforces the one-sampling-period delay. With no modifications of the control scheme, the position controller literally *tracks the past values*. The block diagram for problem is in Fig. 11.

Some delay-compensation schemes have been proposed in the literature for the general visual servoing setup. A particular research motivation comes through a development of a control system for an airborne camera platforms wherein the cameras are exposed to unwanted yet measured motions of the carrier. The inner feedback loop sampled at 200 Hz uses MEMS (Coriolis) gyros to measure the inertial angular rate of the optical payload and struggles to make the deviation from a

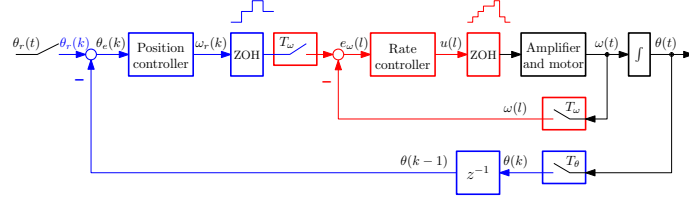


Figure 11: Case A: Problem definition – Cascade visual servoing structure: The inner (velocity, rate) loop works at a fast sampling rate. The outer position (or pointing) loop works at a slow rate and suffers from a one-sampling-period delay.

reference rate small. The outer feedback loop uses an industrial PC to compute the pointing error by finding the deviations in the image plane of the camera, and keeps this error small by commanding the reference value for the inertial angular rate. The computation carried by the image recognition system takes about 1/10 s, but for more advanced computer vision algorithms the computation can easily take up to 2 s.

4.2 Intuitive way of delay compensation

Realizing that the orientation (angle) controller receives measurements that are as old as one full sampling period T_θ , a simple solution comes into an engineer's mind: take an advantage of availability of the angular velocity measurements³, which are available many times (about 10 up to 500 times) during the slow outer loop sampling period. Integrating the frequently arriving values over the slow sampling period gives the desired correction that needs to be subtracted from the outdated measurements coming from the image-based orientation sensor as shown in Fig. 12. The orientation controller then needs to compensate for a smaller error than the image-based sensor suggests. Two variants of this scheme are possible.

4.2.1 Updating at the slow sampling rate (Case B)

The estimates $\hat{\theta}(t)$ of the angle $\theta(t)$ are only updated once the new measurements from the computer vision subsystem arrive, that is, at times $t_k = kT_\theta$, $k \in \mathbb{Z}$. Then the estimated value is fixed over the whole interval $[t_k, t_{k+1})$. It can be calculated according to the Fig. 12 as

$$\hat{\theta}(t_k) = \theta(t_{k-1}) + \underbrace{\int_{t_{k-1}}^{t_k} \omega(\tau) d\tau}_{\Delta\theta(t_k)}, \quad (7)$$

where $\theta(t_{k-1})$ is a crude estimate of the current angle at t_k taken as the delayed measurement performed at t_{k-1} , and $\Delta\theta(t_k)$ is the integrated rate over the full last sampling period T_θ , which makes the crude estimate more accurate.

The block diagram is in Fig. 12. The rate integrator must be periodically reset at all t_k 's, when new position measurements arrive. This can be formally stated as

$$\dot{\Delta}_\theta(t) = \omega(t), \quad \text{for } t \neq t_k, k \in \mathbb{Z}, \quad (8)$$

$$\Delta_\theta(t_k^+) = 0, \quad \text{for } t = t_k, k \in \mathbb{Z}, \quad (9)$$

³It must be emphasized that it is the angular velocity of the camera that is measured. This scheme is therefore particularly useful when the camera is carried by a mobile carrier.

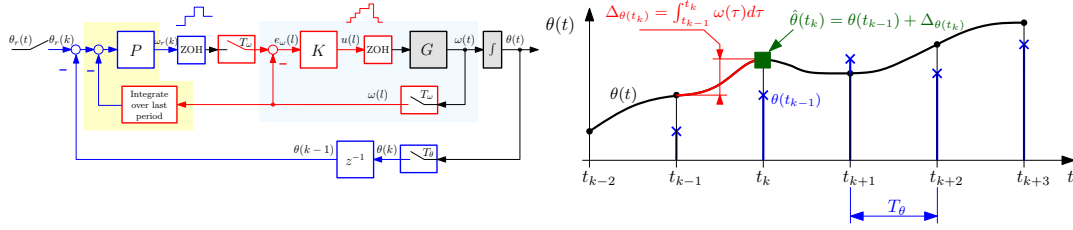


Figure 12: On the left: Case B – Intuitive solution to the problem of having a slow outer loop with a one-period delay: integrate the (undelayed and fast sampled) angular velocity signal ω over one *slow* sampling period T_θ and subtract from the computed orientation (angle) error once the delayed data $\theta(t_{k-1})$ from the computer-vision based sensor arrive. The two blocks in the yellow region now constitute the position controller.

On the right: Case B – The best estimate $\hat{\theta}(t_k)$ at time t_k is obtained from the last known position measurement $\theta(t_{k-1})$ plus the integral of the gyro signal over the last period (the red curve).

where the notation $\Delta\theta(t_k^+)$ stands for $\lim_{t \downarrow t_k} \Delta\theta(t_k)$. This estimate is then used for the full next period.

This heuristic solution turns out efficient when implemented on a real experimental system. A scholarly challenge is to see whether and how this intuitive solution can be formulated using formal concepts from control theory. The major motivation is to use such formalization to find a hint for improving the performance even more, perhaps by exploiting some less intuitive property of the problem.

Resetting the velocity integrator is reminiscent of *reset control* methodology for control design for linear systems, which was introduced by [16] in late 1950s. Its development was documented in the recent surveys [17] and [18] and illustrated by the case studies [19] and [20]. The key principle of reset control is that reset of some controller states is triggered by a certain value of the measured signal. In the simplest case, the integrator in a PI controller is reset (set to zero) every time the regulation error signal crosses zero. When properly designed, the reset controller can beat some restrictions imposed on linear systems such as the water bed phenomenon (Bode integral theorems).

To adapt the reset control formalism to the present problem, it is crucial to realize that the integrator here is reset periodically, independently of values of any measured signal. Such situation was studied in [21]. In this thesis, it is the observer that is periodically reset.

4.2.2 Updating at the fast sampling rate (Case C)

In the previous solution, the estimated position $\hat{\theta}(t)$ is only updated at the slow sampling rate $1/T_\theta$. However, with the measurements arriving from the rate sensor at a much faster rate $1/T_\omega$, it is more efficient to update $\hat{\theta}(t)$ at this faster rate. An estimate $\hat{\theta}(t)$ at time t may be calculated as a sum of the just arrived one-sampling-period old position measurement $\theta(t_{k-1})$ and the numerical integral of the gyro signal as explained in Fig. 13

$$\hat{\theta}(t) = \theta(t_{k-1}) + \underbrace{\int_{t_{k-1}}^t \omega(\tau) d\tau}_{\Delta\theta(t)}. \quad (10)$$

To implement this equation one may reset the integrator every time t_k , when the new measured

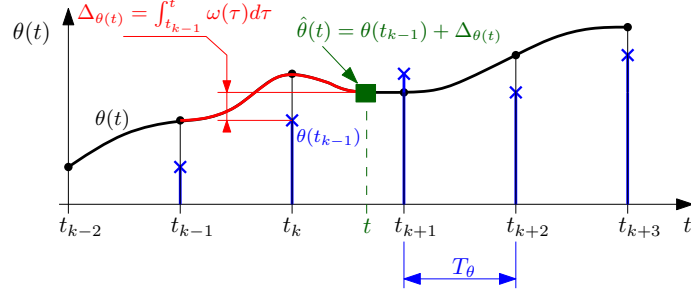


Figure 13: Case C: Time diagram explaining the reset system formulation of the observer of angle. The best estimate $\hat{\theta}(t)$ at time t is obtained from last known position measurement $\theta(t_{k-1})$ plus numerical integral of the gyro signal represented by the red curve. The integration interval thus “breathes”.

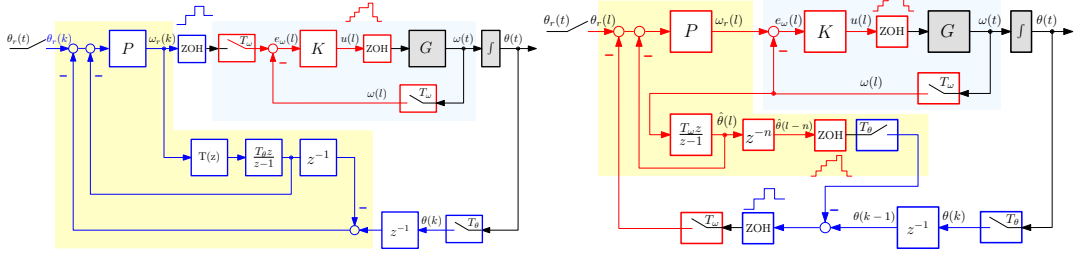


Figure 14: On the left: Smith compensator used in a cascade visual servomechanism. On the right: Case E – Resulting scheme with modified Smith compensator with added re-sampling term.

orientation (angle) arrives. However, do not reset to zero but just subtract $\hat{\theta}(t_{k-1}^+)$ from the integrated value $\hat{\theta}(t_k^-)$ right before the hit of sampling clock. The interval of integration can then be viewed as if *breathing*, that is stretching from one full sampling period to two periods, and shrinking back

$$\dot{\Delta}_{\theta}(t) = \omega(t), \quad \text{for } t \neq t_k, k \in \mathbb{Z}, \quad (11)$$

$$\Delta_{\theta}(t_k^+) = \Delta_{\theta}(t_k^-) - \Delta_{\theta}(t_{k-1}^+), \quad \text{for } t = t_k, k \in \mathbb{Z}. \quad (12)$$

4.3 Modified Smith predictor

With delays in the loop, one is directed to the well-known formal technique of Smith predictor (or compensator). The essence of Smith predictor is to include a model of a delayed system in the controller. Application of this concept to visual servoing is in Fig. 14. The inner closed-loop (red color for signals) is described by the transfer function $T(s)$ from the reference velocity ω_r (as produced by the position controller) to the true velocity ω as measured (neglecting the effect of noise and bias for the moment). Ideally this should be close to one, at least within the bandwidth of the velocity loop. Resampling to the slower sampling period T_{θ} (and abusing the notation by using the same letter T), the transfer function $T(s)$ is viewed as $T(z)$ by the slow controller.

A major deficiency of Smith compensator is its sensitivity to discrepancies between the model and the reality. In particular, if the system is subject to an unmeasured disturbance, the compensator is not aware of it and the performance is deteriorated. Modified Smith predictor has been proposed

in literature, see [22, 23, 24], though it is difficult to give a proper credit to its inventor. The key idea is that when some other variable is also measured on the system, why not use it to make the output of the Smith predictor more accurate? In particular, if the rate (velocity) variable is measured for the purpose of rate stabilization in a cascade feedback configuration, why not use it in place of the output of the model $T(z)$ in the Smith compensator. To exploration of the idea of modified Smith predictor is devoted section 7.3 in the thesis. The best result is achieved with the structure as visualized in Fig. 14.

Comparing all the four compensation schemes mentioned so far, it can be concluded that all of them are based on integration of the rate signal. The intuitive *integrate-over-last-period* solution integrates over the fixed-length interval $[t_{k-1}, t_k)$ and keeps the estimate unchanged for the whole interval $[t_k, t_{k+1})$. The modified reset scheme integrates over an interval that stretches from $[t_{k-1}, t_k)$ to $[t_{k-1}, t_{k+1})$ and then shrinks to $[t_k, t_{k+1})$. The Smith-predictor based compensator performs the integration over the continuously moving window (interval) of the width T_θ .

4.4 Numerical simulations

In order to demonstrate the usefulness of proposed delay compensation schemes, numerical simulations were carried out in Simulink. For this purpose the elevation gimbal model from the double gimbal was used. The model was introduced in section 2.2 in the thesis and identified parameters are listed in table 2.1 in the thesis. Detailed information about the simulation parameters are stated in the thesis in section 6.5. Here only the main result are shown in a form of two graphs in Fig. 15(a) and Fig. 15(b).

The task for the controller is to track a step of 1 rad in the reference angle. System responses under the same conditions with proposed compensator formulated via reset control systems and comparing to the situation when no compensation is applied at all. Apparently, the control design must be rather conservative if no delay compensation is included and larger overshoot is not acceptable.

5 CONCLUSION

The proposed doctoral thesis documents a comprehensive investigation of various research topics that are all related to the task of inertial stabilization of the camera mounted on a mobile carrier, typically an aircraft. The thesis presented a few contributions that were published at prestigious international conferences such as IEEE CDC and IFAC World Congress and a few papers (two accepted, one submitted) at solid journals such as IEEE Transactions on Control Systems Technology, IFAC Mechatronics and IFAC Control Engineering Practice.

The scope of the thesis was fairly wide, the included topics are diverse as visual servoing, delay compensation, structured MIMO controller design and inertial estimation. This character of the doctoral research (and finally the thesis) was certainly shaped by fact that a development of series of inertially stabilized platforms was under way in the supervisors group (in collaboration with other groups including industrial partners). This helped to keep the research focused on relevant problems and provided a unique opportunity to test the results of the work in a very realistic environment, including flight tests.

Whereas in this thesis a few problems lying at the intersection between an inertial stabilization and visual servoing were systematically investigated, it seems promising to explore similarly the area at the intersection between the unmanned aerial vehicle (UAV) path planning and the onboard

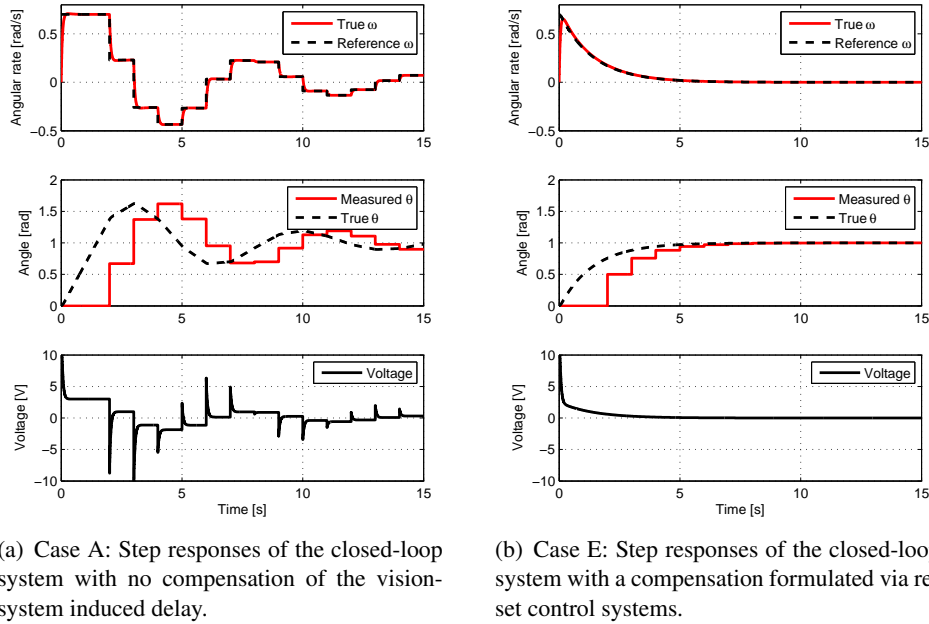


Figure 15: Numerical simulations of delay compensation schemes.

camera pointing and visual tracking. This could immediately initiate a new research thread in the area of UAV path planning, wherein the planning of the path of the UAV is realized in such a way that the tracked object remains observed, that is, well in the camera field of view and in desirable distance. Considering that the camera can be rotated around two or more axes adds new degrees of freedom into the optimization task. In other words, instead of commanding the UAV to *visit* this and that point on a map, the task is to *observe* this and that object.

A few more pragmatic control related issues remain in the list as well. The ever annoying issue of friction in the joints/gimbals is apparently the number one among them. Unlike in most motion control applications here the special feature is that the system mostly operates in the velocity region close to zero. The Stribeck effect is then pronounced. A perfect mechanical design can alleviate a lot of these troubles, nonetheless, armed with the modern control theory tools one may be challenged to model and compensate for this friction. The key trouble is, however, that friction is a relative phenomenon, that is, it is associated with a relative motion of a rotor with respect to the stator, the inner gimbal with respect to the outer gimbal. Unfortunately, our inertial stabilization loops are always based on absolute velocity measured by gyros! Incorporating measurements of the relative velocities of the gimbals in the inertial angular rate stabilization loops is a challenge that does not appear to be discussed in the literature.

References

- [1] J. M. Hilkert, "Inertially stabilized platform technology: concepts and principles," *Control Systems Magazine, IEEE*, vol. 28, pp. 26–46, Feb. 2008.
- [2] Z. Hurák and M. Řezáč, "Combined line-of-sight inertial stabilization and visual tracking: application to an airborne camera platform," in *Proc. of the 48th IEEE Conference on Decision and Control*, Shanghai, China, December 2009.

- [3] —, “Control design for image tracking with an inertially stabilized airborne camera platform,” in *Proc. of SPIE Deference, Security, and Sensing 2010*, Orlando, Florida, USA, April 2010.
- [4] M. Řezáč and Z. Hurák, “Vibration rejection for inertially stabilized double gimbal platform using acceleration feedforward,” in *2011 IEEE International Conference on Control Applications (CCA)*. IEEE, Sep. 2011, pp. 363–368.
- [5] —, “Low-cost inertial estimation unit based on extended kalman filtering,” in *Automatic Target Recognition XX; Acquisition, Tracking, Pointing, and Laser Systems Technologies XXIV; and Optical Pattern Recognition XXI*, vol. 7696. Orlando, Florida, USA: SPIE, Apr. 2010, pp. 76 961F–10.
- [6] M. Masten and L. Stockum, Eds., *Selected Papers on Precision Stabilization and Tracking Systems for Acquisition, Pointing and Control Applications*, ser. SPIE Milestone Series, vol. MS 123. SPIE, 1996.
- [7] M. Masten, “Inertially stabilized platforms for optical imaging systems: Tracking dynamic dynamic targets with mobile sensors,” *Control Systems Magazine, IEEE*, vol. 28, pp. 47–64, Feb. 2008.
- [8] J. Debruin, “Control systems for mobile satcom antennas,” *Control Systems Magazine, IEEE*, vol. 28, pp. 86–101, 2008.
- [9] J. Osborne, G. Hicks, and R. Fuentes, “Global analysis of the double-gimbal mechanism,” *Control Systems Magazine, IEEE*, vol. 28, pp. 44–64, 2008.
- [10] A. Rue, “Stabilization of precision electrooptical pointing and tracking systems,” *Aerospace and Electronic Systems, IEEE Transactions on*, vol. AES-5, pp. 805–819, 1969.
- [11] —, “Precision stabilization systems,” *Aerospace and Electronic Systems, IEEE Transactions on*, vol. AES-10, pp. 34–42, 1974.
- [12] Z. Hurák and M. Řezáč, “Image-based pointing and tracking for inertially stabilized airborne camera platform,” *IEEE Transactions on Control Systems Technology*, vol. 20, no. 5, pp. 1146–1159, Sep. 2012.
- [13] M. W. Spong, S. Hutchinson, and M. Vidyasagar, *Robot Modeling and Control*. Wiley, 2006.
- [14] Z. Hurák and M. Řezáč, “Delay compensation in a dual-rate cascade visual servomechanism,” in *Proc. of the 49th Conference on Decision and Control*, Atlanta, GA, USA, December 2010.
- [15] M. Řezáč and Z. Hurák, “Structured mimo \mathcal{H}_∞ design for dual-stage inertial stabilization: Case study for hifoo and hinfstruct solvers,” Accepted for publishing in *Mechatronics* on 23rd August 2013.
- [16] J. Clegg, “A nonlinear integrator for servomechanisms,” *Trans. AIEE*, vol. 77, no. Part II, pp. 41–42, 1958.
- [17] O. Beker, C. V. Hollot, Y. Chait, and H. Han, “Fundamental properties of reset control systems,” *Automatica*, vol. 40, no. 6, pp. 905–915, Jun. 2004.
- [18] Y. Chait and C. V. Hollot, “On Horowitz’s contributions to reset control,” *International Journal of Robust and Nonlinear Control*, vol. 12, no. 4, pp. 335–355, 2002.

- [19] D. Wu, G. Guo, and Y. Wang, "Reset Integral-Derivative control for HDD servo systems," *Control Systems Technology, IEEE Transactions on*, vol. 15, no. 1, pp. 161–167, 2007.
- [20] Y. Zheng, Y. Chait, C. V. Hollot, M. Steinbuch, and M. Norg, "Experimental demonstration of reset control design," *Control Engineering Practice*, vol. 8, no. 2, pp. 113–120, Feb. 2000.
- [21] Y. Guo, Y. Wang, L. Xie, and J. Zheng, "Stability analysis and design of reset systems: Theory and an application," *Automatica*, vol. 45, no. 2, pp. 492–497, Feb. 2009.
- [22] T. Sim, G. Hong, and K. Lim, "Multirate predictor control scheme for visual servo control," *Control Theory and Applications, IEE Proceedings*, vol. 149, no. 2, pp. 117–124, 2002.
- [23] R. Ergon, "Modified Smith-predictor multirate control utilizing secondary process measurements," *Modeling, identification and control*, vol. 28, no. 1, pp. 15–18, 2007.
- [24] H. Xie, L. Sun, W. Rong, and X. Yuan, "Visual servoing with modified Smith predictor for micromanipulation tasks," in *Mechatronics and Automation, 2005 IEEE International Conference*, vol. 1, 2005, pp. 71–76 Vol. 1.

Abstract

This thesis addresses few various sub-topics that are all related together by the topic of inertial stabilization of the optical axis (so called line-of-sight stabilization) for airborne camera systems. In the first part the thesis provides a brief introduction to main principles of the line-of-sight stabilization followed by description of mathematical models for common mechanical configurations such as double-gimbal and dual-stage configurations. Using these models the control algorithms for the line-of-sight stabilization are derived for all mechanical configurations. The second part of the thesis presents the core of author's research achievements related to the topic. Line-of-sight stabilization is extended for a novel image-based pointing-tracking feedback control scheme with real-time computer vision system. The key idea is to enhance the intuitive decoupled controller structure with measurements of the camera inertial angular rate around its optical axis. Since real-time video processing always introduces one sampling period delay in the vision loop, thesis presents several delay compensation schemes based on modified Smith predictor and reset observer approaches. All the algorithms are always implemented in one of the available benchmark systems (inertially stabilized camera platforms) and tested by laboratory or helicopter flight experiments.

Abstrakt

Tato práce se zabývá několika různými tématy, jež dohromady spojuje téma inerciální stabilizace optické osy pro (bez)pilotní kamerové systémy. Úvodní část práce obsahuje stručné vysvětlení základních pojmů z oblasti stabilizace optické osy, následuje popis matematických modelů pro nejběžnější mechanická uspořádání jako jsou elevace-azimut (angl. double-gimbal) nebo uspořádání s dvojitými závěsy (angl. dual-stage). Tyto modely jsou použity pro odvození řídicích algoritmů pro stabilizaci optické osy. Druhá část práce představuje těžiště autorových výsledků v oboru. Stabilizace optické osy je rozšířena o algoritmus směřování a sledování s využitím obrazové informace z kamery v reálném čase. Základní myšlenka je založena na vylepšení intuitivních řídicích algoritmů na bázi dvou nezávislých SISO regulátorů o využití informace o otáčení kamery okolo své optické osy. Zpracování video-signálu v reálném čase však s sebou vždy přináší nevýhodu ve formě výpočetního zpoždění. To se prakticky projeví v jednokrokovém zpoždění v obrazové řídicí smyčce. Tato práce ukazuje několik možností kompenzace zpoždění založených na principech modifikovaného Smithova prediktoru či resetovaných pozorovatelů. Všechny prezentované algoritmy jsou vždy implementovány v jednom z dostupných vyvíjených systémů (stabilizovaných kamerových základnách) a testovány jak v laboratorních podmínkách tak i v reálném prostředí letových experimentů na vrtulníku.